

Article

Not peer-reviewed version

---

# Preparation of an Cation Exchange Membrane by Sol-Gel Method Based Pva to Improve Alkali Recovery via Diffusion Dialysis in Textile Industry

---

[Jun Yao](#) , Zhenghan Zhang , Haiyang Shen , [Congliang Cheng](#) \*

Posted Date: 12 June 2023

doi: 10.20944/preprints202306.0785.v1

Keywords: alkali recovery; diffusion dialysis; PVA, cationic precursor; sol-gel



Preprints.org is a free multidiscipline platform providing preprint service that is dedicated to making early versions of research outputs permanently available and citable. Preprints posted at Preprints.org appear in Web of Science, Crossref, Google Scholar, Scilit, Europe PMC.

Copyright: This is an open access article distributed under the Creative Commons Attribution License which permits unrestricted use, distribution, and reproduction in any medium, provided the original work is properly cited.

## Article

# Preparation of an Cation Exchange Membrane by Sol-gel Method Based PVA to Improve Alkali Recovery via Diffusion Dialysis in Textile Industry

Jun Yao <sup>1</sup>, Zhenghan Zhang <sup>2</sup> and Haiyang Shen <sup>3</sup>, Congliang Cheng <sup>3,\*</sup>

<sup>1</sup> Department of Modern Garment Engineering, Anhui Vocational And Technical College, Hefei 230011, PR China

<sup>2</sup> Jiangsu FangZheng Plastic Co., Ltd, Suqian, 223900, PR China

<sup>3</sup> School of Materials & Chemical Engineering, Anhui Jianzhu University, Hefei 230022, PR China

\* Correspondence: cclp@mail.ustc.edu.cn

**Abstract:** In this work, a novel silane coupled cationic precursor (SAGS) was synthesized by 3-glycidyloxypropyltrimethoxysilane and sodium 2-((2-aminorthyl)amino) ethanesulfonate. A series of cation exchange membranes were prepared with poly(vinyl alcohol) (PVA) and SAGS by sol-gel process. The structure of the prepared membranes were characterized by fourier transform infrared spectrum (FTIR) and scanning electron microscopy (SEM), and its properties were studied by water uptake ( $W_R$ ), cation exchange capacity (CEC), linear expansion ratio (LER), alkali stability, thermogravimetric analysis (TGA), mechanical properties and diffusion dialysis performance. FTIR and X-ray photoelectron spectroscopy (XPS) confirmed the successful preparation of SAGS membranes, and SEM images showed that the prepared membranes were dense and uniform. The  $W_R$  values of the SAGS membranes were in the range of 91.49-122.39 %, and the LER values were 17.65-28.21 %. In addition, the SAGS membranes had suitable CEC value, good alkali resistance and thermal stability which ensured the application of membranes in the field of diffusion dialysis (DD) for alkali recovery. In DD test, the dialysis coefficients of NaOH ( $U_{OH}$ ) ranged from 0.012 mm/h to 0.023 mm/h, and the separation factors (S) was in the range of 30.77-16.43. In summary, the prepared membrane had good performance and simple preparation process, which had great application potential in textile industrial wastewater recovery.

**Keywords:** alkali recovery; diffusion dialysis; PVA; cationic precursor; sol-gel

## 1. Introduction

In the textile industry, sodium tungstate ( $Na_2WO_4$ ) is commonly used as fabric weighting agent in the production process of fireproof artificial silk [1] and waterproof artificial cotton [2], which can effectively improve the waterproof and fireproof performance of artificial silk or cotton [3–5]. But it is accompanied by the production of a large amount of  $Na_2WO_4$  and sodium hydroxide (NaOH) wastewater [6–8]. Due to massive NaOH in the wastewater, the recovery and reuse of NaOH have significant economic and social significance [9–12]. Diffusion dialysis is one of the most effective ways to treat the wastewater, which includes  $Na_2WO_4$  and NaOH [13–16]. Diffusion dialysis has the advantages of low energy consumption, good separation effect and simple process [15–17]. The key core of recovery NaOH via diffusion dialysis is to prepare high-performance cation exchange membranes (CEM) [18–23]. The cation exchange membrane (CEM) mainly contains fixed groups (such as sulfonate or carboxyl group) and dissociable ions, which can be dissociated from fixed groups, and make the membrane with negative charge [20–23]. The CEM with negative charge can be selectively through the cation and block anions. Preparation of high-performance cation exchange membranes has been the unremitting pursuit of many scholars [21–26].

CEM could be mainly divided into two types: the first type was heterogeneous ion exchange membrane, such as semi-interpenetrating network structure of cation exchange membrane, blending polymer cation exchange membrane [27–30]; The other type was homogeneous ion exchange membrane, such as sulfonated polyether ether ketone [31,32], sulfonated polyphenyl ether [33,34],

perfluorosulfonic acid membrane (Nafion) [35,36]. The performance requirements of CEM should contain the following three characteristics: 1. High ion permeability flux and selectivity. This required that the membrane not only has appropriate water content, but also has good barrier property to anion [26,37,38]. 2. Outstanding thermal stability, mechanical stability and low swelling degree. The performance of membrane decreased in the long-time application process, so it was necessary to maintain the performance stability of the separation process in a long period of time [27,39]. 3. Good alkali resistance. For diffusion dialysis, cation exchange membranes adopting traditional polymers as the backbone can no longer meet the requirement of long-term stability under strong alkaline condition, which was also difficult for commercialization of recovery alkaline via diffusion dialysis [40]. High-performance cation exchange membranes had many problems such as cumbersome preparation methods, unfriendly environment, high price and limited application environment [23–26]. Hence, it was the pursuit of the majority of ion exchange membrane researchers to prepare cation exchange membranes with simple preparation, environmentally friendly process and excellent performance.

At present, CEMs based on Polyvinyl alcohol (PVA) are studied intensively [41,42]. For example, Y H. Wu et al. prepared cation exchange hybrid membranes with blending SPPO in PVA/SiO<sub>2</sub> matrix [43], the PVA improved the hydrophilicity of the hybrid membrane, and the ion flux of CEM increased. Chunhua Dai et al. prepared hybrid cation exchange membrane by combining benzaldehyde disulfonic acid disodium salt with PVA [44], the results showed that the prepared cation exchange membranes had good performance [11]. There were also a lot of literature on the preparation of CEMs with PVA. The main reason is that polyvinyl alcohol was a new green material with low price, environmental friendliness, wide compatibility and good alkali resistance, which have attracted the interest of most researchers. So PVA was often used to prepared CEM.

In this paper, a silane coupling agent containing an epoxy group was used to react with an amino-containing sulfonate to synthesize a silane coupling agent with sulfonate group (SAGS) [45], and then the cation exchange membrane was prepared with PVA and SAGS by sol-gel reaction. The preparation process was carried out in the aqueous phase, which was environmentally friendly. At the same time, the performance of the prepared membrane was comprehensively studied, which provided technical support for recovery NaOH via diffusion dialysis in the recycling wastewater in the textile industry.

## 2. Materials and Methods

### 2.1. Materials

Polyvinyl alcohol (PVA) and dimethyl sulfoxide (DMSO) were purchased from Sinopharm Chemical Reagent (Shanghai, China), and the average degree of PVA was  $1750 \pm 50$ . 3-glycidyloxypropyltrimethoxysilane(97%) and sodium 2-((2-aminorthyl)amino)ethanesulfonate(50% in H<sub>2</sub>O) were supplied by Shanghai Macklin Biochemical Technology Co., Ltd (Shanghai, China).

### 2.2. Methods

#### 2.2.1. Synthesis of SAGS

As shown in Figure 1, SAGS was synthesized by the reaction of 3-glycidyloxypropyltrimethoxysilane and 2-((2-aminorthyl)amino)- ethanesulfonate. First, 1.36 g(0.005 mol) 3-glycidyloxypropyltrimethoxy- silane and 16.64 g DMSO were loaded in a dried 50 ml round-bottomed flask with adequately stirring at 80 °C in order to completely mix. After 30 min, 2.00 g 2-((2-aminorthyl)amino)- ethanesulfonate was slowly added dropwise into the mixed solution and then the mixture was continue stirred at 80 °C for 6 hours to fully react. The product was a colorless transparent viscous solution in DMSO.

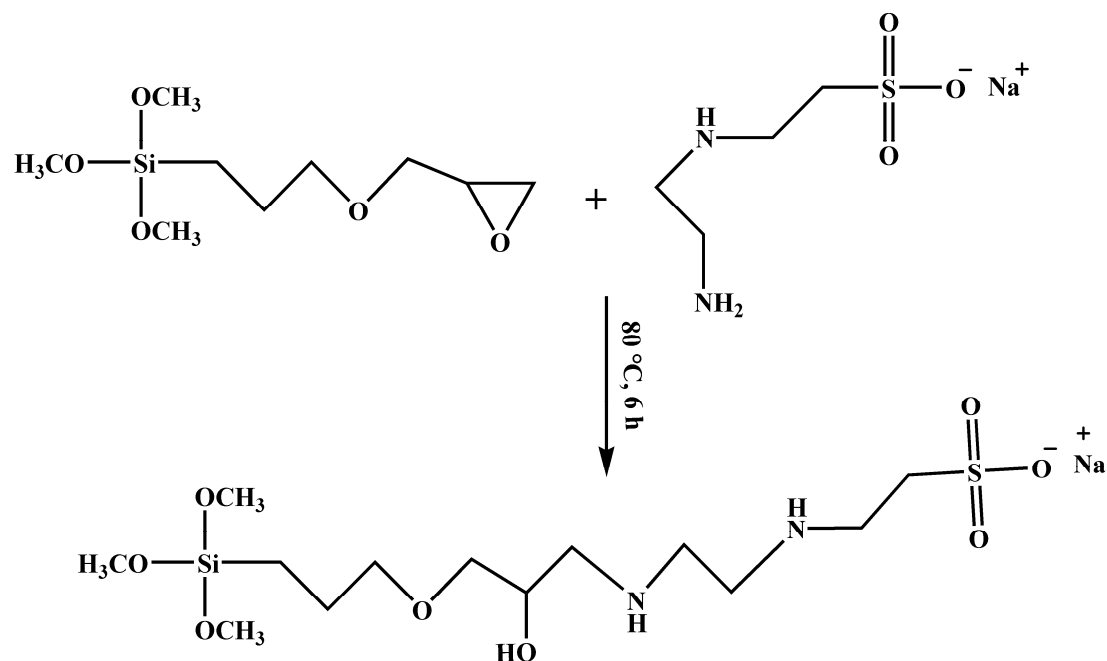


**Figure 1.** Synthesis scheme of the silane coupling agent with sulfonate group (SAGS).

### 2.2.2. Preparation of SAGS-X cation exchange membrane.

The preparation process of SAGS-X cation exchange membrane is shown in Figure 2. First, PVA was completely dissolved using DMSO at 90 °C to prepare 5 wt% PVA solution. Second, the SAGS solution was added into the PVA solution to according to different mass ratios (SAGS to PVA: 16%, 32%, 48%, 64% and 80%). The sol-gel reaction was for 24 hours at 60 °C. The solution after the sol-gel reaction was cast on a clean glass plate and dried in a vacuum oven at 60 °C to form membrane. After the solvent has fully evaporated, the membrane was detached from the plate and then the membrane was heated in vacuum oven at 110 °C for 4 hours to make membrane completely cross-linking. Finally, the membrane was stored in deionized water for further testing. The prepared membranes were named SAGS-X, where X represented the mass percentage of SAGS in PVA.

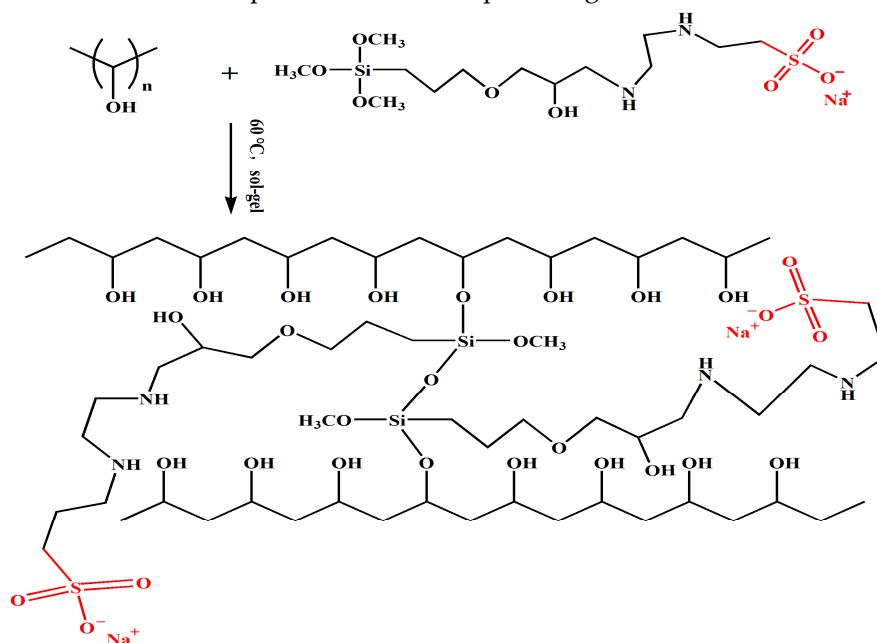


**Figure 2.** Synthesis scheme of the SAGS-X cation exchange membranes.

### 2.3. SEM, TGA, FTIR, XPS

Chemical functional groups information of the SAGS-X cation exchange membranes was obtained by Fourier transform infrared spectroscopy (FTIR, Nicolet 6700, Thermo Fisher Scientific of American). FTIR condition was set with a resolution of 0.1 cm<sup>-1</sup> and a wavenumber range of 4000-400 cm<sup>-1</sup>. The surface elemental compositions of prepared membranes were analyzed by X-ray photoelectron spectroscopy (XPS, Escalab 250Xi) measurements. The cross-section microstructure analysis of the SAGS-X cation exchange membranes was performed by scanning electron microscopy (SEM, JSM-7500F, JEOL of Japan). Thermal stability of the SAGS-X cation exchange membranes was obtained by thermogravimetric analysis (TGA, TGA-50H, Shimadzu of Japan). TGA condition was set with a constant heating ratio of 10°C per minutes from room temperature to 600°C under N<sub>2</sub> atmosphere.

### 2.4. Water uptake ( $W_R$ )

Water uptake ( $W_R$ ) was measured by standard method below. Primarily, the SAGS-X CEM was dried to constant weight, and recorded the weight in the dry state ( $W_{dry}$ ) by analytical balance, and then the membrane was completely immersed in deionized water for 48 hours at room temperature. After wiping off the surface moisture, the membrane was weighed again and recorded the weight ( $W_{wet}$ ) of in a fully absorbed moisture state. Water uptake ( $W_R$ ) that based on the data obtained above was calculated, and the formula is as follows.

$$W_R = \frac{W_{wet} - W_{dry}}{W_{dry}} \times 100 \quad (1)$$

### 2.5. Cation exchange capacity (CEC) and the thickness of the membrane

The cation exchange capacity (CEC) of the SAGS-X CEM was determined by studying the content of -SO<sub>3</sub>H groups in membrane under dry weight conditions. Theoretical value of CEC ( $CEC_T$ ) was obtained through theoretical simulation calculation. Experimental value of CEC ( $CEC_E$ ) was characterized by titration method. First, the dried SAGS-X CEM was accurately weighed by analytical balance ( $W_{Dry}$ ). And then the membrane was equilibrated with 1 M HCl aqueous solution for 48 hours to convert to H<sup>+</sup> form. Afterwards the membrane was washed with DI water for three times in order to completely remove the residual acid, and finally put into 0.04 M NaCl aqueous solution for 48 hours. The content of H<sup>+</sup> which was released by the membrane was tested through titration with 0.04 M NaOH aqueous solution to determine cation exchange capacity. The CEC (mmol·g<sup>-1</sup>) was calculated as follows.

$$CEC = \frac{C_{NaOH} V_{NaOH}}{W_{Dry}} \quad (2)$$

Where  $C_{NaOH}$  was the concentration of the NaOH aqueous solution, and  $V_{NaOH}$  was the volume of the NaOH aqueous solution.

The thickness of the membrane used spiral micrometer to measure.

### 2.6. Linear expansion ratio (LER) and alkali stability

Linear expansion ratio (LER) was important properties to evaluate dimensional stability of cation exchange membrane. The membrane in the dry state was cut into a rectangular shape with a length of 5 cm and a width of 1 cm. LER test was similar to the  $W_R$  test, the membrane lengths in both dry and wet states were recorded before and after the test. LER was calculated as follows.

$$LER = \frac{L_{wet} - L_{dry}}{L_{dry}} \times 100 \quad (3)$$

Alkali stability was a key property of CEM to estimate membrane application performance. The weight of the membrane in the dry state was firstly recorded. After that, the membrane was immersed into 2 M NaOH aqueous solution for 168 hours at room temperature. Finally, the membrane was washed, dried, and weighed again. The weight maintenance rate was calculated as the ratio of the



mass of the membrane before and after the acid resistance test which was a main indicator to evaluate the alkali stability of the membrane.

### 2.7. Diffusion dialysis (DD)

At first, the prepared SAGS-X CEM was immersed in feed solution (1 M NaOH+0.1 M Na<sub>2</sub>WO<sub>4</sub>) which was used to simulate waste water for 2 hours. Next, the membrane needed to be washed carefully for several times with the use of DI water. Then the membrane was placed in the experimental device which was the combination of two compartments. These two compartments were separated by the prepared membrane, and the effect area between two parts was 5.5 cm<sup>2</sup>. Based on the work above, 100 mL DI water was poured into one compartment and 100 mL feed solution was put into the other compartment. After that, in order to minimize concentration polarization, both compartments needed to be strongly stirred for 60 minutes. Later, 10 ml solution from each compartment of the experimental device was removed. OH<sup>-</sup> concentration in the solution was determined by titration with HCl solution, while WO<sub>4</sub><sup>2-</sup> concentration was determined by thiocyanate spectro photometric method. The calculation of dialysis coefficients (U) and separation factors (S) was calculated as follows.

$$U = \frac{M}{At\Delta C} \quad (4)$$

where M was the amount of component transported in moles, A was the effective area in square meters, t was the time in hours, and  $\Delta C$  was the logarithmic mean of the concentration difference between the two chambers,  $\Delta C$  can be calculated as below.

$$\Delta C = \frac{c_f^0 - (c_f^t - c_d^t)}{\ln[c_f^0 - (c_f^t - c_d^t)]} \quad (5)$$

where  $C_f^0$  and  $C_f^t$  were the feed concentrations at time 0 and t, respectively and  $C_d^t$  was the dialysate concentration at time t.

The separation factor (S) of membrane was calculated using the ratio of dialysis coefficients (U) of the two species (WO<sub>4</sub><sup>2-</sup> and OH<sup>-</sup>) presented in the solution. S can be calculated as below.

$$S = \frac{U_{OH}}{U_{WO_4^{2-}}} \quad (6)$$

The data obtained from W<sub>R</sub>, LER, CEC, DD performance, and film thickness had been tested for an average of three times.

## 3. Results and discussion

### 3.1. FT-IR

The chemical structure information of membranes SAGS-16, SAGS-32, SAGS-48, SAGS-64 and SAGS-80, which was studied by FT-IR (Figure 3). The large and wide bands at 3600-3200 cm<sup>-1</sup> was the tensile vibration peaks of hydroxyl in PVA and SAGS [45]. The peaks that appeared at 2937 cm<sup>-1</sup> and 2907 cm<sup>-1</sup> were due to the symmetric and asymmetric stretching vibration peaks of methylene [46]. The absorption peak at 1646 cm<sup>-1</sup> was ascribed to the bending vibration peak of the hydroxyl groups on the sulfonic groups [44]. The uptake peaks at 1420 cm<sup>-1</sup> and 1323 cm<sup>-1</sup> were due to the bending vibration peaks of methylene and the rocking vibration peaks of hydroxyl groups, respectively[44]. The absorption peak at 1191 cm<sup>-1</sup> was assigned to the S=O asymmetric vibration peak of -SO<sub>3</sub>H groups [46]. The S-O stretching vibration peak of -SO<sub>3</sub>H groups was also clearly observed at 1041 cm<sup>-1</sup>[46]. The presence of -SO<sub>3</sub>H groups in the membranes could be fully confirmed by the characteristic absorption peaks of -SO<sub>3</sub>H groups which appeared at 1191 cm<sup>-1</sup> and 1041 cm<sup>-1</sup>. The stretching vibration of Si-O-Si and Si-O-C appears at 1018 cm<sup>-1</sup>, and these groups mainly formed by the sol-gel process.

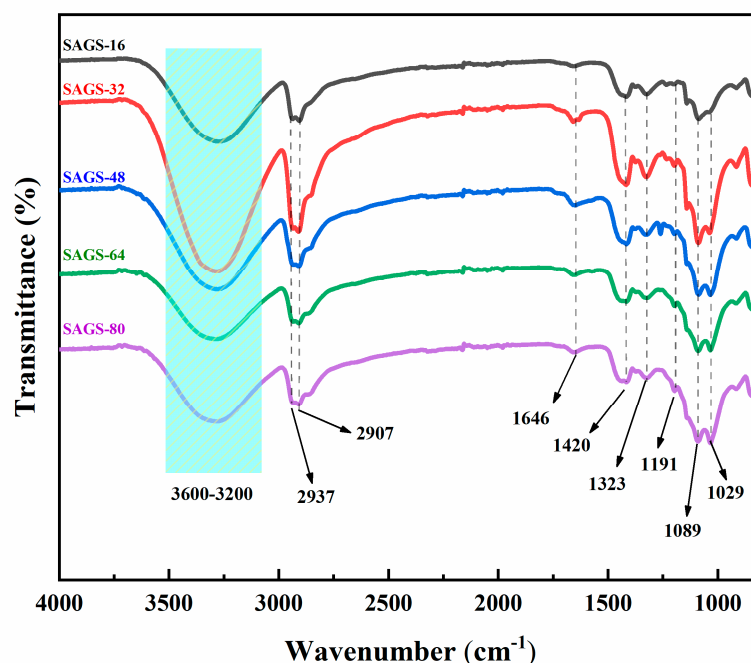


**Figure 3.** FTIR spectra of the SAGS-X cation exchange membranes.

### 3.2. Thermal stability

Thermal stability of the SAGS-X CEMs was evaluated using TGA and DTG. According to Figure 4, the weight loss process of the SAGS-X CEM was divided into three decomposition stages. In the first decomposition stage, the main loss of membranes was the free water and bound water in the membrane in the temperature range of 80-120 °C [13]. The second decomposition stage occurring from 280 °C to 310°C was mainly the degradation of grafted side chain functional groups such as -SO<sub>3</sub>H groups [47]. The mass loss in the last decomposition temperature which was from 370-480 °C was due to mainly from the degradation of the polymer backbone [48]. According to the TGA curve, the residual mass of the prepared membranes gradually increased from SAGS-16 to SAGS-80. Therefore, the addition of SAGS which could increase the overall crosslinking degree of the membrane significantly improved the thermal stability of the prepared membranes. The initial decomposition temperature (IDT) of the SAGS membranes was 266.6-282.5 °C, and thermal degradation temperature ( $T_d$ ) was in the ranged of 278.5 °C to 283.9 °C from Table 1. So that, the IDT and  $T_d$  values of the SAGS-X CEMs were completely higher than the operating temperature of the CEM.

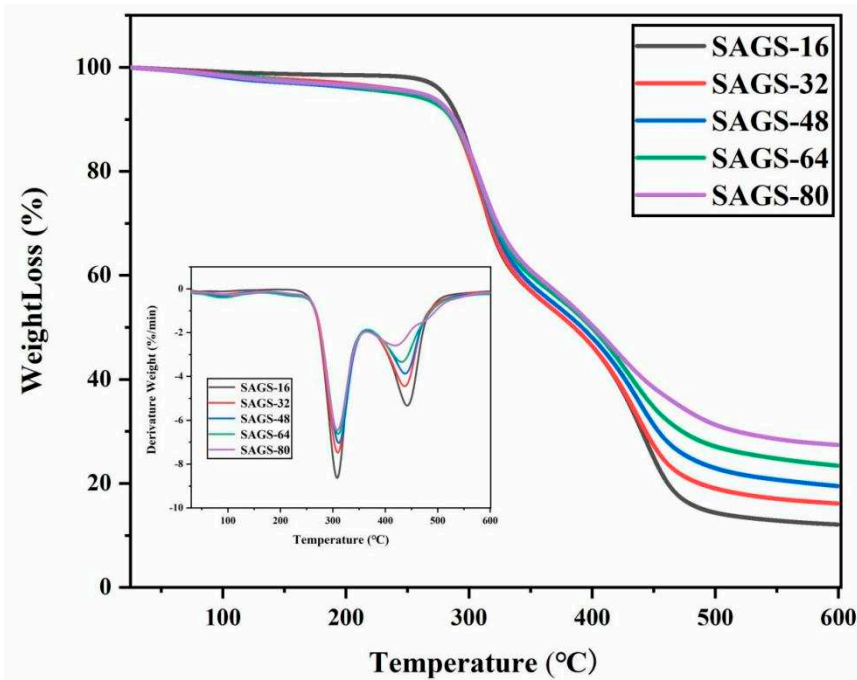


Figure 4. TGA and DTG curves of the SAGS-X cation exchange membranes.

Table 1. IDT and T<sub>d</sub> values of the SAGS-X cation exchange membranes.

Membrane	SAGS-16	SAGS-32	SAGS-48	SAGS-64	SAGS-80
IDT (°C) <sup>a</sup>	266.6	268.4	271.5	266.8	282.5
T <sub>d</sub> (°C) <sup>b</sup>	283.9	278.5	280.3	278.7	282.5

<sup>a</sup> IDT is the initial decomposition temperature determined from TGA thermograms. <sup>b</sup> Thermal degradation temperature (T<sub>d</sub>) is defined as the temperature at which the weight loss becomes 5% in TGA thermograms.

3.3. XPS Spectra of Membranes

In order to obtained more comprehensive structural information of prepared membrane, the surface chemical component of the membrane was determined by XPS. The test results of membranes are shown in the Figure 5.

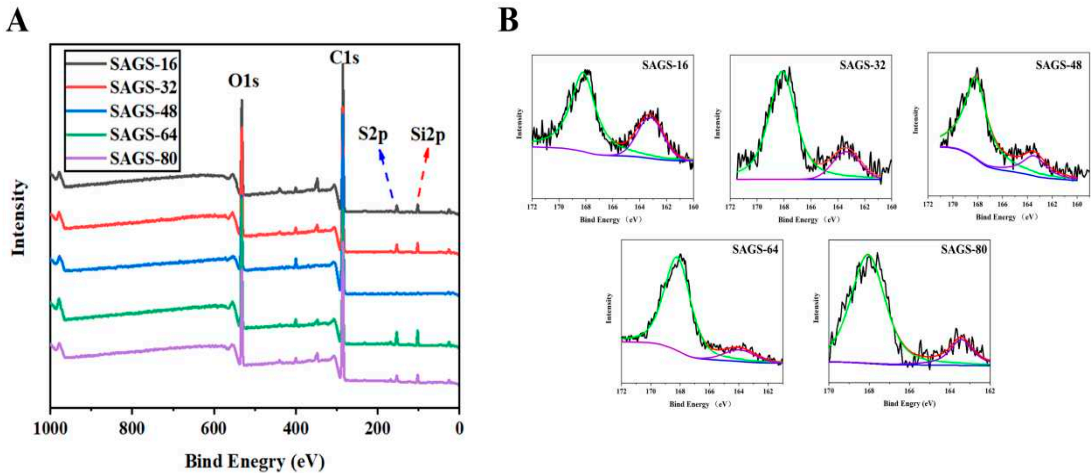


Figure 5. (A) XPS spectra of prepared membranes; (B) high-resolution S 2p spectra of prepared membranes.



The peak at 532 eV was O 1s. This peak was related to -OH on the PVA chain and -O- in the silane coupling agent[49]. The peak at 102 eV was Si 2p, which confirmed the presence of Si bond in the membrane[49].

In addition, the success synthesized of membrane can be supported by the high-resolution spectra of S 2p. taking membrane SAGS-16 as an example, the XPS signal can be clearly deconvoluted into two peaks in Figure 7B. The two peak detected at 168.2 eV and 163.5 eV in Figure 7B was related to the S atom in the sulphonic group[50].

3.4. Water uptake ( $W_R$ ), linear expansion ratio (LER) and cation exchange capacity (CEC).

The water uptake of the SAGS CEM was tested to collect data, which shown in the table 2. The  $W_R$  value of the membrane was 91.49-122.39%. The increased of  $W_R$  value was due to the strong hydrophilicity of the sulfonic acid group. The content of SAGS in the membrane increased, the number of sulfonic acid groups also enhanced, which resulting in an increase in the water uptake of the membrane. The increased content of SAGS made polar groups increased, and resulting in the formation of larger ion clusters, which would cause the membrane to absorb more water and increased the  $W_R$  value. The LER value of the membrane was 17.65-28.21% (Table 2). The enhanced of LER was due to the SAGS content increased, which improved the crosslinking degree of the membrane and enhanced the dimensional stability [46]. The number of ion exchange groups of the prepared membrane was determined by the CEC value. The CEC of the prepared membrane was estimated by using the titration method, and the results were shown in Table 2. The CEC value was 0.25-0.84 mmol/g. The CEC value mainly depends on the number of sulfonic acid groups present in the membrane. With the increased content of SGAS, the number of sulfonic acid groups raised, and the CEC value of the membrane increased. The thickness of the SAGS cation membrane was 91-112  $\mu\text{m}$ . Compared with other membranes, as shown in Table 3. The experimental membrane had good CEC value, lower LER value.

**Table 2.**  $W_R$ , LER and CEC of the SAGS-X cation exchange membranes.

Membrane	SAGS-16	SAGS-32	SAGS-48	SAGS-64	SAGS-80
$W_R$	91.49	94.34	96.67	112.31	122.39
LER	17.65	24.42	26.51	27.32	28.21
$CEC_T$	0.36	0.64	0.85	1.03	1.17
$CEC_E$	0.25	0.42	0.57	0.72	0.84
Thickness( $\mu\text{m}$ )	99	91	103	112	107

**Table 3.** Ion exchange capacity (CEC), water uptake ( $W_R$ ), and linear expansion ratio (LER) values of different membranes.

Membrane	CEC(mmol/g)	$W_R(\%)$	LER (%)	Ref.
SAGS-X	0.25-0.84	91.49-122.39	17.65-28.21	This work
PVA/TiO <sub>2</sub>	0-0.0157	90.9-101.7	187.2-206.5	[51]
PVA/CBAC <sub>5</sub>	0.0147-0.0518	122.6-150	222.6-241.9	[52]

### 3.5. Mechanical properties and alkali resistance

Mechanical properties were the material properties of CEMs. The TS and  $E_b$  values were shown in Figure 6. The tensile strength (TS) of the membrane was 20.1-30.8 MPa, and elongation at break ( $E_b$ ) value was 92.3-107.2%. Due to the stronger molecular force caused by the cross-linking of the polymer chains, which improved the mechanical properties of the membrane, enhanced the value of TS and  $E_b$  of the membrane[53,54]. For SAGS-80, TS and  $E_b$  values of the membrane decreased attribute to excessive crosslinking of the membrane, which lead to uneven stress distribution of the membrane and excessive hardness of the local membrane, thereby affecting the TS and  $E_b$  values of the membrane [54,55]. Compared with other reported membranes, the prepared membranes had good TS and  $E_b$  values. The relevant data was shown in Table 4.

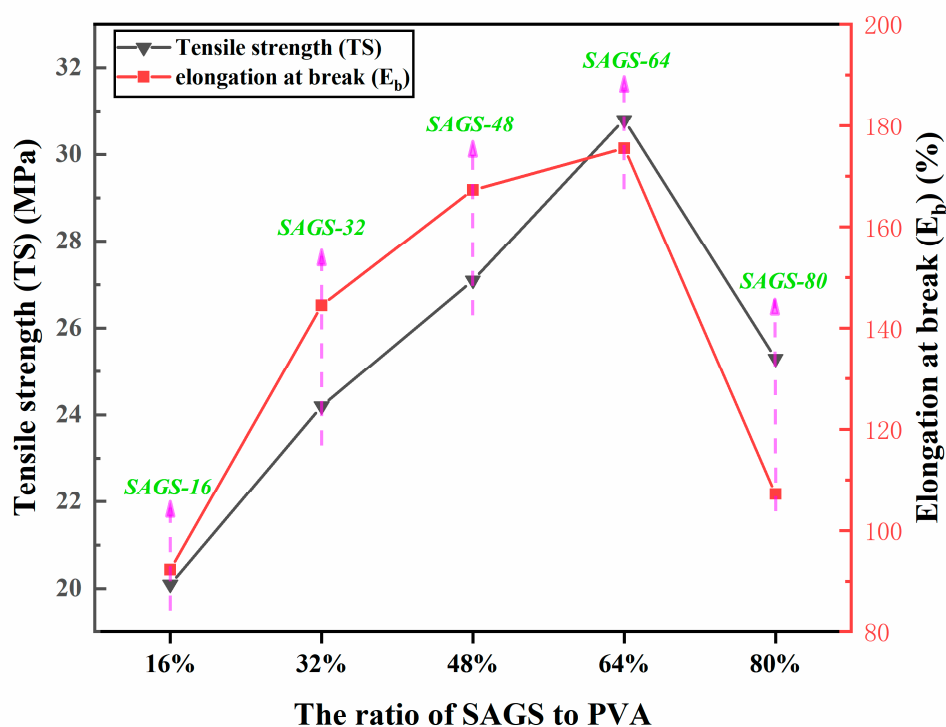


**Figure 6.** Tensile strength (TS) and elongation at break ( $E_b$ ) of the SAGS-X cation exchange membranes.

**Table 4.** TS and  $E_b$  values of different membranes.

Membrane	TS(MPa)	$E_b$ (%)	Ref.
SAGS-X	20.1-30.8	92.3-107.2	This work
PVA/SSS/ $\gamma$ -MPS	9.1-26.0	12.4-21.1	[56]
PVA/SPPO	12-13	27-49	[54]
PVA/MA/ $\gamma$ -MPS	14.2-28.3	18.8-67.3	[57]

### 3.6. Alkali resistance

The alkali resistance of the membrane reflected its potential application in the field of diffusion dialysis for alkali recovery. The membrane was immersed in a 2 M NaOH environment at 25 °C for 168 hours, and weight maintenance of the membrane was tested. The weight maintenance of the membrane was shown in Table 5. The weight maintenance of the SAGS-X CEM was above 88%. The

data showed that the SAGS-X CEM had good alkali resistance that was suitable for application in the field of diffusion dialysis for alkali recovery.

**Table 5.** Weight maintenance of the SAGS-X cation exchange membranes.

Membrane	SAGS-16	SAGS-32	SAGS-48	SAGS-64	SAGS-80
Weight maintenance (%)	91.4	94.3	88.3	90.2	91.9

3.7. Membrane morphologies

With the use of SEM, the homogeneity and uniformity of five prepared membranes could be researched detailly. The cross-sectional morphologies of obtained membranes were presented in Figure 7. According to the SEM images, it was not difficult to observe that the membranes were dense and compact without any volume and cracks, which was mainly attributed to the cross-linking between PVA and SAGS. And with the increase of SAGS in membrane, more SAGS cross linked with PVA, which led to increased membrane compactness. It also could be observed that the phenomenon of particle aggregation. Those white dots appeared in images were the silica particles in membrane [54]. Taking SAGS-80 as an example, the membrane with highest SAGS content, showed the most obvious aggregation due to the accelerated hydrolysis of silica precursor. In addition, the SAGS-64 and SAGS-80 showed the slight phase separation, which was of great help to improve the diffusion dialysis performance for alkali recovery [45].

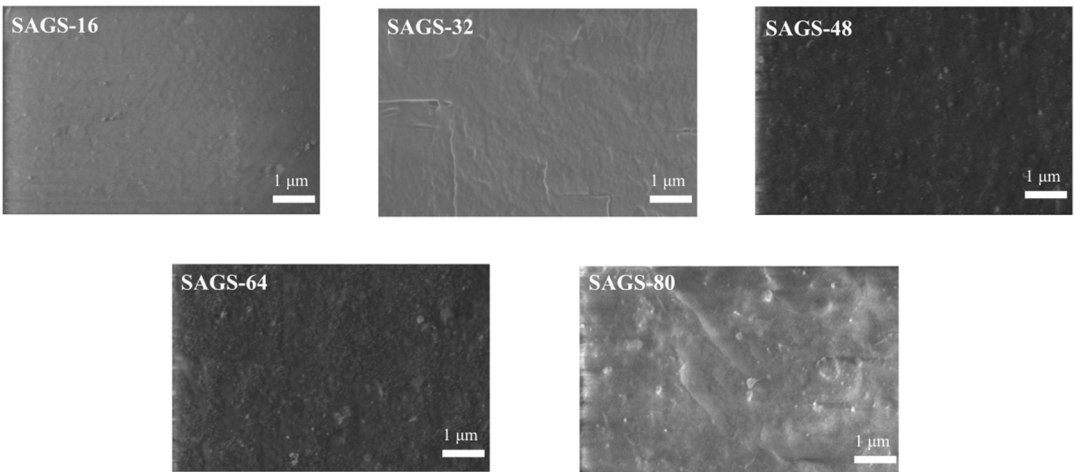


**Figure 7.** The morphology of the SAGS-X cation exchange membranes by SEM.

3.8. Diffusion dialysis (DD)

The performance of diffusion dialysis was vital for anion exchange membranes, which was about whether the prepared membranes could be used in industrial production and daily life. Thus the diffusion dialysis experiment was carried out by taking NaOH/Na<sub>2</sub>WO<sub>4</sub> mixture (1.0 M NaOH/0.1 M Na<sub>2</sub>WO<sub>4</sub>) as the feed solution, and relevant experimental results were shown in the Figure 8.

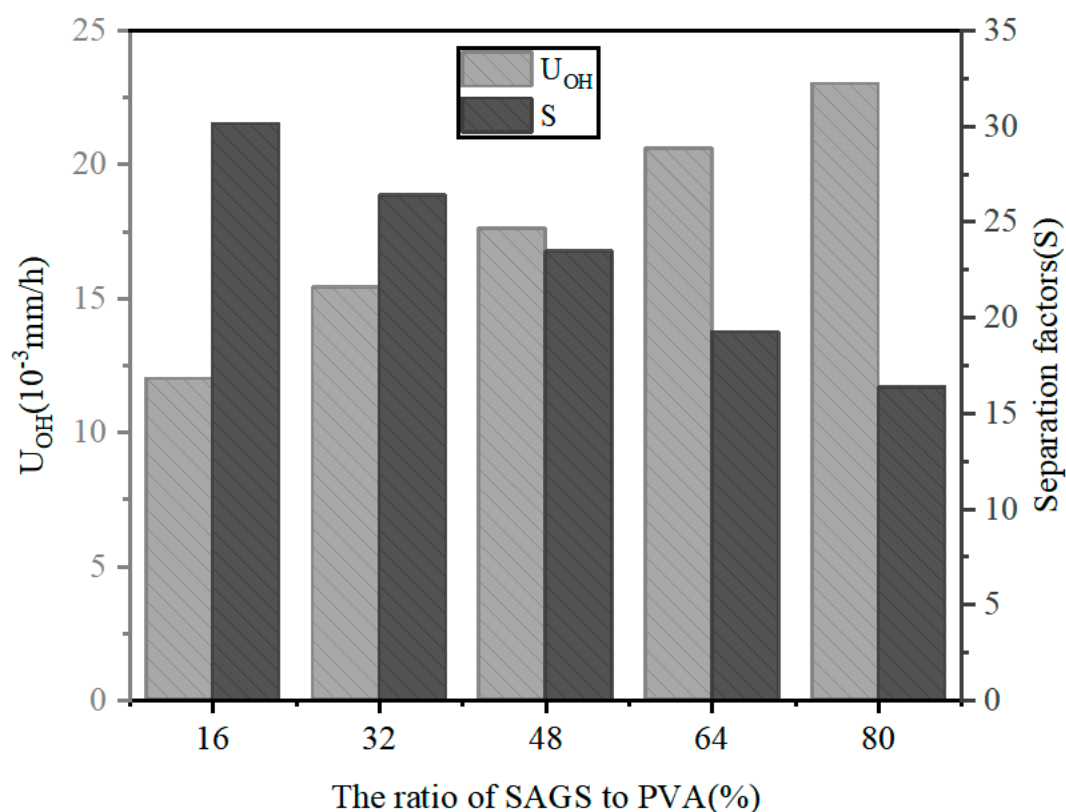


**Figure 8.**  $U_{OH}$  and S of membrane SAGS-X cation exchange membranes.

From the collected data,  $U_{OH^-}$  value was increased from 0.012 mm/h to 0.023 mm/h with the increase of SAGS content. That was mainly due to the  $-SO_3H$  groups carried the negative charge, so  $OH^-$  and  $WO_4^{2-}$  groups which carried the same charge were hardly pass through the cation exchange membranes [52]. On the contrary, those cations in feed solution can be easily transported to the side. For the sake of meeting the requirement of electric neutrality, anions also must be migrated. Compared with  $WO_4^{2-}$ ,  $OH^-$  had less charge and the size of  $OH^-$  was smaller, which resulted in that the  $U_{OH^-}$  value gradually increased. Secondly, the increased CEC and  $W_R$  had an effect on the performance of diffusion dialysis [45]. Both these two showed an upward trend, which had a positive effect on ion migration, hence the increase in  $U_{OH}$  values.

The  $U_{WO_4^{2-}}$  value ranged from  $0.39 \times 10^{-3}$  mm/h to  $1.40 \times 10^{-3}$  mm/h. Under the condition that the membrane structure became more and more dense, the reason for the increase of  $U_{WO_4^{2-}}$  value was phase separation [55]. Based on the previous discussion, more larger ion channels appeared on the membrane because of phase separation, which indicated that  $WO_4^{2-}$  groups could pass through the membrane easily. The increased IEC and  $W_R$  also promoted the migration of  $WO_4^{2-}$  same as  $OH^-$  groups. However, this migration of  $WO_4^{2-}$  was not conducive to membrane selectivity, which caused the decrease of S value.

The S value was the ratio of  $U_{OH^-}$  and  $U_{WO_4^{2-}}$ , and the value was in the range of 30.77-16.43. Compared with some membranes previously reported, the prepared membranes showed the higher separation factor (13.6-18.1) [53], (16.9-18.5) [57]. In order to better prove the changes in different ion transport properties caused by the changes in the internal structure of the membrane, the internal transport mechanism diagram based on the corresponding data was drawn and shown in Figure 8. Compared with other membranes, the prepared membrane had good S value. The relevant data was shown in Table 6.

**Table 6.** The  $U_{OH}$  and S values of different membranes.

Membrane	$U_{OH}(10^{-3}m/h)$	S	Ref.
SAGS-X	12-23	16.43-30.77	This work
PVA/SSS	11-19	13.6-18.1	[53]
PVA/ $\gamma$ -MPS/SSS	10.2-11.1	16.9-18.5	[57]
PVA/THOPS	11-22	11.6-20.6	[59]

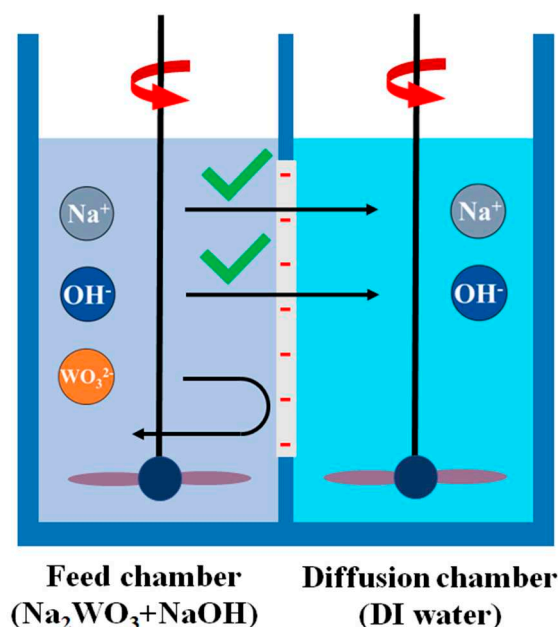


**Figure 9.** the internal transport mechanism diagram of the SAGS-X cation exchange membranes.

#### 4. Conclusions

A series of long side chain PVA based cation exchange membranes had been successfully prepared by sol-gel process. The SAGS membrane had moderate  $W_R$  and LER, suitable CEC value, and excellent alkali stability. Moreover, the SAGS membrane had extremely high thermal stability and a microstructure conducive for diffusion dialysis. In DD test, the  $U_{OH}$  and S value of the SAGS membrane were in the range of 0.012-0.023 mm/h and 16.43-30.77, respectively. When the content of SAGS reached 80%, the membrane had a maximum  $U_{OH}$  value (0.023 mm/h) and a minimum S value (16.34). Hence, these good properties indicated that the membrane had certain application potential in the field of DD for alkali recovery.

**Acknowledgments:** This work was supported by Natural Science Foundation of Anhui Provincial, China(1908085MB55), Natural Science Foundation of Anhui Provincial Education, China(KJ2020ZD44), Science and Technology Projects of Anhui Province, China(202103c08020001).

#### References

1. Liu, L.; Ma, Z.; Zhu, M.; Liu, L.; Dai, J.; Shi, Y.; Gao, J.; Dinh, T.; Nguyen, T.; Tang, L.-C.; et al. Superhydrophobic self-extinguishing cotton fabrics for electromagnetic interference shielding and human motion detection. *J. Mater. Sci. Technol.* **2023**, *132*, 59-68
2. Wang, S.; Du, X.; Luo, Y.; Lin, S.; Zhou, M.; Du, Z.; Cheng, X.; Wang, H. Hierarchical design of waterproof, highly sensitive, and wearable sensing electronics based on MXene-reinforced durable cotton fabrics. *Chem. Eng. J.* **2021**, *408*, 127363.
3. Krishnan, S.A.G.; Gumpu, M.B.; Arthanareeswaran, G.; Goh, P.S.; Aziz, F.; Ismail, A.F. Electrochemical quantification of atrazine-fulvic acid and removal through bismuth tungstate photocatalytic hybrid membranes. *Chemosphere* **2023**, *311*, 137016.
4. Krishnan, S.A.G.; Sasikumar, B.; Arthanareeswaran, G.; László, Z.; Nascimben Santos, E.; Veréb, G.; Kertész, S. Surface-initiated polymerization of PVDF membrane using amine and bismuth tungstate (BWO) modified MIL-100(Fe) nanofillers for pesticide photodegradation. *Chemosphere* **2022**, *304*, 135286.

5. Yang, Y.; Fan, H.; Wu, T.; Yang, G.; Han, B. Complete degradation of high-loaded phenol using tungstate-based ionic liquids with long chain substituent at mild conditions. *Green Energy Environ.* **2023**, *8*, 452-458.
6. Li, B.; Shu, J.; Wu, Y.; Su, P.; Yang, Y.; Chen, M.; Liu, R.; Liu, Z. Enhanced removal of  $Mn^{2+}$  and  $NH_4^+-N$  in electrolytic manganese residue leachate by electrochemical and modified phosphate ore flotation tailings. *Sep. Purif. Technol.* **2022**, *291*, 120959.
7. Li, X.; Miao, J.; Xia, R.; Yang, B.; Chen, P.; Cao, M.; Qian, J. Preparation and properties of sulfonated poly (2, 6-dimethyl-1, 4-phenyleneoxide)/mesoporous silica hybrid membranes for alkali recovery. *Microporous Mesoporous Mater.* **2016**, *236*, 48-53.
8. Zhang, X.; Zhang, X.; An, C.; Wang, S. Electrochemistry-enhanced peroxydisulfate activation by CoAl-LDH@biochar for simultaneous treatment of heavy metals and PAHs. *Sep. Purif. Technol.* **2023**, *311*, 123341.
9. Zhang, X.; Niu, J.; Hao, X.; Wang, Z.; Guan, G.; Abudula, A. A novel electrochemically switched ion exchange system for phenol recovery and regeneration of NaOH from sodium phenolate wastewater. *Sep. Purif. Technol.* **2020**, *248*, 117125.
10. Zhao, Y.; Wang, X.; Yuan, J.; Ji, Z.; Liu, J.; Wang, S.; Guo, X.; Li, F.; Wang, J.; Bi, J. An efficient electrodialysis metathesis route to recover concentrated NaOH- $NH_4Cl$  products from simulated ammonia and saline wastewater in coal chemical industry. *Sep. Purif. Technol.* **2022**, *301*, 122042.
11. Chen, T.; Bi, J.; Ji, Z.; Yuan, J.; Zhao, Y. Application of bipolar membrane electrodialysis for simultaneous recovery of high-value acid/alkali from saline wastewater: An in-depth review. *Water Res.* **2022**, *226*, 119274.
12. Deng, S.; Wang, C.; Ngo, H.H.; Guo, W.; You, N.; Tang, H.; Yu, H.; Tang, L.; Han, J. Comparative review on microbial electrochemical technologies for resource recovery from wastewater towards circular economy and carbon neutrality. *Bioresour. Technol.* **2023**, *376*, 128906.
13. Chen, W.; Shen, H.; Gong, Y.; Li, P.; Cheng, C. Anion exchange membranes with efficient acid recovery obtained by quaternized poly epichlorohydrin and polyvinyl alcohol during diffusion dialysis. *J. Membr. Sci.* **2023**, *674*, 121514.
14. You, X.; Chen, J.; Pan, S.; Lu, G.; Teng, L.; Lin, X.; Zhao, S.; Lin, J. Piperazine-functionalized porous anion exchange membranes for efficient acid recovery by diffusion dialysis. *J. Membr. Sci.* **2022**, *654*, 120560.
15. Liu, B.; Duan, Y.; Li, T.; Li, J.; Zhang, H.; Zhao, C. Nanostructured anion exchange membranes based on poly(arylene piperidinium) with bis-cation strings for diffusion dialysis in acid recovery. *Sep. Purif. Technol.* **2022**, *282*, 120032.
16. Yan, J.; Wang, H.; Fu, R.; Fu, R.; Li, R.; Chen, B.; Jiang, C.; Ge, L.; Liu, Z.; Wang, Y.; et al. Ion exchange membranes for acid recovery: Diffusion Dialysis (DD) or Selective Electrodialysis (SED)? *Desalination* **2022**, *531*, 115690.
17. Lin, J.; Huang, J.; Wang, J.; Yu, J.; You, X.; Lin, X.; Van der Bruggen, B.; Zhao, S. High-performance porous anion exchange membranes for efficient acid recovery from acidic wastewater by diffusion dialysis. *J. Membr. Sci.* **2021**, *624*, 119116.
18. Park, J.; Ko, Y.-j.; Lim, C.; Kim, H.; Min, B.K.; Lee, K.-Y.; Koh, J.H.; Oh, H.-S.; Lee, W.H. Strategies for  $CO_2$  electroreduction in cation exchange membrane electrode assembly. *Chem. Eng. J.* **2023**, *453*, 139826.
19. Fujimura, Y.; Kawakatsu, T.; Morimoto, M.; Asakawa, H.; Nakagawa, K.; Yoshioka, T. Study for removing of silica nanoparticle in pure isopropyl alcohol with a cation exchange membrane. *J. Mol. Liq.* **2022**, *367*, 120441.
20. Nazif, A.; Saljoughi, E.; Mousavi, S.M.; Karkhanechi, H. Improved permselectivity and mechanical properties of sulfonated poly dimethyl phenylene oxide cation exchange membrane using MXene nanosheets. *Desalination* **2023**, *549*, 116329.
21. Pahnavar, Z.; Ghaemy, M.; Naji, L.; Hasantabar, V. Self-extinguished and flexible cation exchange membranes based on modified K-Carrageenan/PVA double network hydrogels for electrochemical applications. *Int. J. Biol. Macromol.* **2023**, *231*, 123253.
22. Li, C.; Song, K.; Hao, C.; Liang, W.; Li, X.; Zhang, W.; Wang, Y.; Song, Y. Fabrication of S-PBI cation exchange membrane with excellent anti-fouling property for enhanced performance in electrodialysis. *Colloids Surf., A* **2023**, *661*, 130910.
23. Zheng, Y.; Jin, Y.; Zhang, N.; Wang, D.; Yang, Y.; Zhang, M.; Wang, G.; Qu, W.; Wu, Y. Preparation and characterization of  $Ti_3C_2Tx$  MXene/PVDF cation exchange membrane for electrodialysis. *Colloids Surf., A* **2022**, *650*, 129556.
24. Xue, J.; Liu, X.; Zhang, J.; Yin, Y.; Guiver, M.; Poly(phenylene oxide)s incorporating N-spirocyclic quaternary ammonium cation/cation strings for anion exchange membranes. *J. Membr. Sci.* **2020**, *595*, 117507.
25. Swanckaert, B.; Locqufier, E.; Geltemeyer, J.; Rabaey, K.; De Buysser, K.; Bonin, L.; De Clerck, K. Sulfonated silica-based cation-exchange nanofiber membranes with superior self-cleaning abilities for electrochemical water treatment applications. *Sep. Purif. Technol.* **2023**, *309*, 123001.
26. Thakur, A.K.; Malmali, M. Advances in polymeric cation exchange membranes for electrodialysis: An overview. *J. Environ. Chem. Eng.* **2022**, *10*, 108295.



27. Kozmai, A.E.; Mareev, S.A.; Butylskii, D.Y.; Ruleva, V.D.; Pismenskaya, N.D.; Nikonenko, V.V. Low-frequency impedance of ion-exchange membrane with electrically heterogeneous surface. *Electrochim. Acta* **2023**, *451*, 142285.
28. Szakács, S.; Koók, L.; Nemestóthy, N.; Bélafi-Bakó, K.; Bakonyi, P. Studying microbial fuel cells equipped with heterogeneous ion exchange membranes: Electrochemical performance and microbial community assessment of anodic and membrane-surface biofilms. *Bioresour. Technol.* **2022**, *360*, 127628.
29. Lee, S.; Meng, W.; Wang, Y.; Wang, D.; Zhang, M.; Wang, G.; Cheng, J.; Zhou, Y.; Qu, W. Comparison of the property of homogeneous and heterogeneous ion exchange membranes during electrodialysis process. *Ain Shams Eng. J.* **2021**, *12*, 159-166.
30. İpekçi, D.; Kabay, N.; Bunani, S.; Altok, E.; Arda, M.; Yoshizuka, K.; Nishihama, S. Application of heterogeneous ion exchange membranes for simultaneous separation and recovery of lithium and boron from aqueous solution with bipolar membrane electrodialysis (EDBM). *Desalination* **2020**, *479*, 114313.
31. Chikumba, F.T.; Tamer, M.; Akyalçın, L.; Kaytakoglu, S. The development of sulfonated polyether ether ketone (sPEEK) and titanium silicon oxide (TiSiO<sub>4</sub>) composite membranes for DMFC applications. *Int. J. Hydrogen Energy* **2023**, *48*, 14038-14052.
32. Lou, X.; Lu, B.; He, M.; Yu, Y.; Zhu, X.; Peng, F.; Qin, C.; Ding, M.; Jia, C. Functionalized carbon black modified sulfonated polyether ether ketone membrane for highly stable vanadium redox flow battery. *J. Membr. Sci.* **2022**, *643*, 120015.
33. Haragirimana, A.; Li, N.; Hu, Z.; Chen, S. A facile, effective thermal crosslinking to balance stability and proton conduction for proton exchange membranes based on blend sulfonated poly(ether ether ketone)/sulfonated poly(arylene ether sulfone). *Int. J. Hydrogen Energy* **2021**, *46*, 15866-15877.
34. Devrim, Y. Fabrication and Performance Evaluation of Hybrid Membrane based on a Sulfonated Polyphenyl Sulfone/Phosphotungstic acid/Silica for Proton Exchange Membrane Fuel Cell at Low Humidity Conditions. *Electrochim. Acta* **2014**, *146*, 741-751.
35. Vrána, J.; Charvát, J.; Mazúr, P.; Bělský, P.; Dundálek, J.; Pociď, J.; Kosek, J. Commercial perfluorosulfonic acid membranes for vanadium redox flow battery: Effect of ion-exchange capacity and membrane internal structure. *J. Membr. Sci.* **2018**, *552*, 202-212.
36. Jung, B.; Moon, H.-M.; Baroña, G.N.B. Effect of methanol on plasticization and transport properties of a perfluorosulfonic ion-exchange membrane. *J. Power Sources* **2011**, *196*, 1880-1885.
37. Pan, J.; Zhao, L.; Yu, X.; Dong, J.; Liu, L.; Zhao, X.; Liu, L. Optimizing functional layer of cation exchange membrane by three-dimensional cross-linking quaternization for enhancing monovalent selectivity. *Chin. Chem. Lett.* **2022**, *33*, 2757-2762.
38. Jalal, N.M.; Jabur, A.R.; Hamza, M.S.; Allami, S. Sulfonated electrospun polystyrene as cation exchange membranes for fuel cells. *Energy Rep.* **2020**, *6*, 287-298.
39. Salma, U.; Shalahin, N. A mini-review on alkaline stability of imidazolium cations and imidazolium-based anion exchange membranes. *Results Mater.* **2023**, *17*, 100366.
40. Thakur, A.K.; Malmali, M. Advances in polymeric cation exchange membranes for electrodialysis: An overview. *J. Environ. Chem. Eng.* **2022**, *10*, 108295.
41. Dong, F.; Xu, S.; Wu, X.; Jin, D.; Wang, P.; Wu, D.; Leng, Q. Cross-linked poly(vinyl alcohol)/sulfosuccinic acid (PVA/SSA) as cation exchange membranes for reverse electrodialysis. *Sep. Purif. Technol.* **2021**, *267*, 118629.
42. Hao, J.; Wu, Y.; Xu, T. Cation exchange hybrid membranes prepared from PVA and multisilicon copolymer for application in alkali recovery. *J. Membr. Sci.* **2013**, *425-426*, 156-162.
43. Wu, Y.; Hao, J.; Wu, C.; Mao, F.; Xu, T. Cation exchange PVA/SPPO/SiO<sub>2</sub> membranes with double organic phases for alkali recovery. *J. Membr. Sci.* **2012**, *423-424*, 383-391.
44. Dai, C.; Mondal, A.N.; Wu, L.; Wu, Y.; Xu, T. Crosslinked PVA-based hybrid membranes containing di-sulfonic acid groups for alkali recovery. *Sep. Purif. Technol.* **2017**, *184*, 1-11.
45. Mondal, A.N.; Zheng, C.; Cheng, C.; Miao, J.; Hossain, M.M.; Emmanuel, K.; Khan, M.I.; Afsar, N.U.; Ge, L.; Wu, L.; et al. Novel silica-functionalized aminoisophthalic acid-based membranes for base recovery via diffusion dialysis. *J. Membr. Sci.* **2016**, *507*, 90-98.
46. Liu, C.-P.; Dai, C.-A.; Chao, C.-Y.; Chang, S.-J. Novel proton exchange membrane based on crosslinked poly(vinyl alcohol) for direct methanol fuel cells. *J. Power Sources* **2014**, *249*, 285-298.
47. Gouda, M.H.; Ellessawy, N.A.; Toghan, A. Development of effectively costed and performant novel cation exchange ceramic nanocomposite membrane based sulfonated PVA for direct borohydride fuel cells. *J. Ind. Eng. Chem.* **2021**, *100*, 212-219.
48. Yang, C.-C. Alkaline direct methanol fuel cell based on a novel anion-exchange composite polymer membrane. *J. Appl. Electrochem.* **2012**, *42*, 305-317.
49. Gong, Y.F.; Chen, W.; Shen, H.Y.; Cheng, C.L. Semi-interpenetrating Polymer-Network Anion Exchange Membrane Based on Quaternized Polyepichlorohydrin and Polyvinyl Alcohol for Acid Recovery by Diffusion Dialysis. *Ind. Eng. Chem. Res.* **2023**, *62*, 5624-5634.

50. Mosa, J.; Duran, A.; Aparicio, M. Sulfonic acid-functionalized hybrid organic-inorganic proton exchange membranes synthesized by sol-gel using 3-mercaptopropyl trimethoxysilane (MPTMS). *J. Power Sources* **2015**, *297*, 208-216.
51. Liang, Y.; Huang, X.; Yao, L.; Xia, R.; Cao, M.; Ge, Q.; Zhou, W.; Qian, J.; Miao, J.; Wu, B. Regulation of Polyvinyl Alcohol/Sulfonated Nano-TiO<sub>2</sub> Hybrid Membranes Interface Promotes Diffusion Dialysis. *Polymers (Basel)* **2020**, *13*.
52. Peng, L.; Huang, X.; Liu, D.; Miao, J.; Wu, B.; Cao, M.; Ge, Q.; Yang, B.; Su, L.; Xia, R.; et al. Preparation of Polyvinyl Alcohol (PVA)-Based Composite Membranes Using Carboxyl-Type Boronic Acid Copolymers for Alkaline Diffusion Dialysis. *Polymers* **2020**, *12*, 2360.
53. Wu, Y.; Gu, J.; Wu, C.; Xu, T. PVA-based cation exchange hybrid membranes with multifunctional groups prepared from ternary multisilicon copolymer. *Sep. Purif. Technol.* **2013**, *104*, 45-54.
54. Ashraf, M.A.; Islam, A.; Butt, M.A. Novel Silica Functionalized Monosodium Glutamate/PVA Cross-Linked Membranes for Alkali Recovery by Diffusion Dialysis. *J. Polym. Environ.* **2021**, *30*, 516-527.
55. Cui, M.B.; Wu, Y.H.; Ran, J.; Xu, T.W. Preparation of cation-exchange hybrid membranes with multifunctional groups and their performance on alkali recovery. *Desalin. Water Treat.* **2015**, *54*, 2627-2637.
56. Ji, W.; Afsar, N.U.; Wu, B.; Sheng, F.; Shehzad, M.A.; Ge, L.; Xu, T. In-situ crosslinked SPPO/PVA composite membranes for alkali recovery via diffusion dialysis. *J. Membr. Sci.* **2019**, *590*, 117267.
57. Gu, J.; Wu, C.; Wu, Y.; Luo, J.; Xu, T. PVA-based hybrid membranes from cation exchange multisilicon copolymer for alkali recovery. *Desalination* **2012**, *304*, 25-32.
58. Wu, C.M.; Gu, J.J.; Wu, Y.H.; Luo, J.Y.; Xu, T.W.; Zhang, Y.P. Carboxylic acid type PVA-based hybrid membranes for alkali recovery using diffusion dialysis. *Sep. Purif. Technol.* **2012**, *92*, 21-29.
59. Hao, J.W.; Wu, Y.H.; Ran, J.; Wu, B.; Xu, T.W. A simple and green preparation of PVA-based cation exchange hybrid membranes for alkali recovery. *J. Membr. Sci.* **2013**, *433*, 10-16.

**Disclaimer/Publisher's Note:** The statements, opinions and data contained in all publications are solely those of the individual author(s) and contributor(s) and not of MDPI and/or the editor(s). MDPI and/or the editor(s) disclaim responsibility for any injury to people or property resulting from any ideas, methods, instructions or products referred to in the content.